Heliyon 10 (2024) e30429

Contents lists available at ScienceDirect

Heliyon

journal homepage: www.cell.com/heliyon

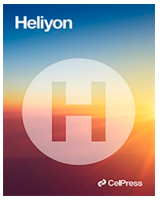

Research article

3D printed lightweight honeycomb vent structures with subsequent coating of silver nanowires for efficient electromagnetic interference (EMI) shielding

Raheel Abbas [a,b,1], Ubaid ur Rehman [a,1], Ahmed bilal [a], Numrah Sultan [a], Uzma Ghazanfar [b], Tahir Ali [c], Muhammad Nadeem [a,*]

[a] Polymer Composite Group, Directorate of Science, PINSTECH, Nilore, 44000, Islamabad, Pakistan
[b] Department of Physics, University of Wah, Wah Rawalpindi, Pakistan
[c] Physics Division, Directorate of Science, PINSTECH, Islamabad, Pakistan

ARTICLE INFO

Keywords:
EMI shielding
Silver nanowires
3D printing
Thermoplastics
Honeycomb structures

ABSTRACT

In light of the rapid advancements within the electronic industry, the urgent need for the development and implementation of advanced electromagnetic interference (EMI) shielding materials has become paramount. Herein a novel approach is presented for developing of lightweight honeycomb structures using 3D printing technology, combined with subsequent conductive spray coating, containing Silver Nanowires (AgNWs), to achieve effective EMI shielding as well as air vent functionality for thermal cooling.

Using polyol method, AgNWs were synthesized having high aspect ratio and crystallinity for to be used as conductive coating on 3D printed structures. The EMI shielding results in X-band demonstrated that the developed structures exhibit promising EMI shielding properties, up to 35 dB attenuation with 2 mm honeycomb cell size, making them suitable for applications requiring EMI protection along with air venting. More importantly in all samples major contribution of the shielding efficiency comes from the absorption of the EM waves (up to 75 %) inside the structures which is helpful to reduce reflected EM noise.

Effort was to effectively addresses the inherent limitations of conventional processing technology, by using additive manufacturing and material science to create structures for EMI shielding applications, bridging the gap between existing materials and desired components.

1. Introduction

Electromagnetic Interference (EMI) has become a pervasive issue in modern electronic systems, leading to performance degradation and malfunctions [1–3]. As the demand for more compact and fast electronic devices continues to rise, the need for effective EMI shielding solutions becomes increasingly critical [1,4,5]. Traditional approaches to EMI shielding, such as metal enclosures (Faraday cages) offer good shielding efficiency in broad range of frequencies but on the other hand often suffer from limitations in weight, weather resistance, flexibility, and manufacturing complexity [6–8]. Therefore, there is a growing interest in exploring

* Corresponding author.
E-mail address: mnadeemsb@gmail.com (M. Nadeem).
[1] These authors contributed equally in this work.

https://doi.org/10.1016/j.heliyon.2024.e30429
Received 28 November 2023; Received in revised form 28 March 2024; Accepted 25 April 2024
Available online 30 April 2024

alternative methods and materials to achieve efficient EMI shielding [9–12].

Another situation arises when both EMI shielding and thermal cooling are necessary for an electronic component [13–18]. In such cases, a lightweight EMI shielding material with integrated vents for air circulation becomes essential [19,20]. However, it is important to note that introducing slots/aperture in a shield can result in a decline in its shielding effectiveness [21]. The extent of this decline is influenced by the size of the holes or slots and the wavelength of the electromagnetic waves being shielded [22–24]. Therefore, it is crucial to determine an optimal vent size that allows for sufficient air circulation to enable effective cooling of the component while providing reliable EMI shielding [25,26]. This dual-functionality makes them particularly suitable for miniaturized and densely packed electronic devices, where traditional EMI shielding methods may be impractical [27].

In recent years, additive manufacturing techniques, particularly 3D printing, have emerged as promising tools for fabricating complex and customizable structures [28–30]. Thanks to the unique additive manufacturing process, 3D printing possesses great advantages in constructing arbitrarily customized geometries via a layer-by-layer stacking manner [31–33]. Utilizing its unique manufacturing methods, 3D printing offers significant potential for creating a wide range of components that are challenging or impossible to produce using conventional processing techniques [34,35]. Numerous innovative structures have been successfully fabricated through 3D printing with customized internal feature [36,37]. Typically in the domain of EMI shielding, when electromagnetic waves (EMWs) penetrate into the interior of the structure they encounter continuous reflection and scattering on the framework of the porous units [38]. This phenomenon leads to the trapping of EMWs within the structure until their energy is absorbed and dissipated as in the form of electromagnetic dipoles relaxation and/or eddy currents losses [27,39,40].

One such structure that has gained attention is the honeycomb lattice, known for its excellent mechanical properties and lightweight nature [41]. Honeycomb structures have been widely utilized in various applications, including aerospace, automotive, and packaging industries, due to their high strength-to-weight ratio and energy absorption capabilities [42]. Harnessing these unique characteristics, researchers have begun exploring the use of 3D printed honeycomb structures for EMI shielding applications [43].

Recent trends in this field focus on the utilization of advanced materials and manufacturing techniques to further enhance the EMI shielding performance of 3D printed honeycomb structures [44–47]. Literature surveys have revealed several studies focusing on the fabrication and characterization of 3D printed honeycomb structures for EMI shielding application, incorporating electromagnetic active nanomaterials [40,48,49]. Researchers have explored different methods to enhance the electromagnetic performance of these structures, including the use of conductive materials and surface treatments [50–52]. One notable trend involves the use of conductive nanomaterials, such as carbon allotropes, MXenes, and metallic nanostructures, which offer high electrical conductivity while maintaining the lightweight and flexible nature of the honeycomb lattice [53–56]. These approaches aim to increase the electrical conductivity of the honeycomb structures, thereby improving their EMI shielding effectiveness [38,57,58]. The incorporation of these nanomaterials within the 3D printing process or as a post-processing step holds great promise for achieving superior EMI shielding efficiency [59].

Silver nanostructures, such as nanoparticles, nanowires, and nanosheets, have gained significant attention as promising materials for electromagnetic interference (EMI) shielding due to their exceptional electrical conductivity and good environmental stability [60,61]. These nanostructures exhibit superior performance in EMI shielding applications compared to traditional bulk silver due to large surface area which provides multiple sites for interaction of electromagnetic waves [62,63]. Among these morphologies, nanowires stand out due to their high aspect ratio, which enables efficient EMI shielding at reduced material thickness [64]. The elongated shape of nanowires provides enhanced electrical conductivity along the axis and larger surface area for the interaction of electromagnetic field, resulting in superior shielding effectiveness [65–67]. Additionally, the use of AgNWs as transparent EMI shielding materials has also been explored [68,69]. The combination of high electrical conductivity and transparency makes AgNWs an ideal candidate for applications where both EMI shielding and optical transparency are desired, such as touch screens, flexible displays, and solar cells [67,70]. AgNWs can be applied as coatings on various materials to render their surfaces conductive, enabling effective EMI shielding [71]. The deposition of AgNWs coatings provides a lightweight and flexible solution for enhancing the conductivity of non-conductive surfaces, such as plastics or glass, while maintaining their transparency and preserving the aesthetic appeal [72,73]. This approach offers a versatile and efficient method for incorporating EMI shielding capabilities into a wide range of materials and applications, including electronic enclosures, medical devices, and automotive components.

In light of the above literature surveys, the presented study aims to investigate the development of 3D printed honeycomb structure as a promising candidate for EMI shielding applications. By merging the utilization of an innovative additive manufacturing technique with conductive nanomaterials like AgNWs, the presented approach establishes a connection between the realms of material science and technology. Specifically, we explored the effect of honeycomb cell size on EMI shielding performance while coating of AgNWs was kept constant. The objective was to create stable lightweight structures that simultaneously facilitate air ventilation and provide reliable EMI shielding. The findings of this research will contribute to advancing the field of EMI shielding by providing novel insights into the material selection, design, fabrication, and characterization of 3D printed honeycomb structures with enhanced electromagnetic performance.

2. .Experimental details

2.1. Materials

For synthesis of AgNWs, the following analytical grade chemicals were used without any further purifications. All chemicals are purchased from commercial sources. **a)** Silver Nitrate ($AgNO_3 > 99.8$ %), **b)** Glycerol ($C_3H_8O_3 > 99$ %) **c)** Poly(vinylpyrrolidone) (PVP K-90), **d)** Sodium Chloride (NaCl > 99.5 %), **e)** Ethanol (C_2H_5OH >99 %).

2.2. Synthesis of Ag nanowire (AgNWs)

High aspect AgNWs were synthesized using hydrothermal method [74–76]. Briefly speaking 23 mmol of PVP was completely dissolved in glycerol by stirring at 100°C. Two other solutions were made by adding 3 mmol of $AgNO_3$ into 10 ml of glycerol at room temperature and 0.062 mmol of NaCl into 20 ml of glycerol at 70°C. All solutions were stirred magnetically until additives were fully dissolved and clear transparent solution was obtained. Following that, silver solution and NaCl solution were slowly added to PVP solution respectively and stirred for 5–10 min. Then the solution was immediately transferred to 200 ml capacity autoclave preheated at 150°C. For the growth of AgNWs the autoclave was placed in oven at 150°C for 6 h s. After the autoclave was cooled down to room temperature 100 ml DI water was added to the solution and AgNWs were collected by centrifugation at 6000 rpm for 10 min. AgNWs were washed several times with DI water and absolute ethanol alternatively to remove undesirable reaction products. Finally, the obtained AgNWs were dispersed in DI water for further use.

2.3. Characterization of AgNWs

The phase identification and crystallite size measurements were performed using RIGAKU DMAX-IIIA JAPAN, with a scan rate of $0.25^{o}/min^{-1}$ from 30° to 90° utilizing Cu-kα radiation. The morphology of AgNWs was observed using field emission scanning electron microscope (TESCAN MAIA-3 (FESEM)), and energy dispersive spectrometry (EDS) was used to analyze the elemental composition.

Figure-1(a) shows the XRD pattern of AgNWs, diffraction peaks are observed at 38.51^0, 44.77^0, 65.17^0. 78.32^0 and 82.54^0 which corresponds to the *hkl* value of (111), (200), (220), (311) and (222) respectively. These values are in agreement with the standard JCPDS 04–0783 card of silver. AgNWs have a face centered cubic crystal structure, and it belongs to Fm-3m space group [77].

Figure-1(b) represents the UV–vis absorption spectrum of AgNWs solution in water. The main absorption band is observed at a λ_{max} of 375 nm, it is associated with the optical signature of AgNWs [78,79]. The peak position of the plasmon resonance in the UV–Vis spectrum of AgNWs is typically red-shifted (shifted to longer wavelengths) compared to silver nanoparticles of similar size. The red-shift arises from the anisotropic shape and extended aspect ratio of the nanowires, which enhance the coupling between electrons and result in a lower resonant frequency [80,81].

SEM and EDS results of AgNWs are shown in Figure-2. A wire like morphology is observed in the SEM images and AgNWs of high aspect ratio are synthesized with a consistent diameter. The average aspect ratio (length to width ratio) of AgNWs is around 230 (~8um:0.035μm). The presence of few clusters was also observed which could be due to the unavailability of PVP molecule at those sites, resulting in the formation of agglomerates instead of wire. EDS spectrum along with XRD analysis indicate that sample prepared has a high purity [79].

2.4. 3D printing of honeycomb structures

Honeycomb structures were manufactured using the Fused Deposition Modeling (FDM) technique, which falls under the category of additive manufacturing. The CAD model of the structures were designed using Blender-2.93.4 software, and the slicing process was performed using Ultimaker Cura software. For printing the structure, Polylactic Acid (PLA) was selected as the printing material due to

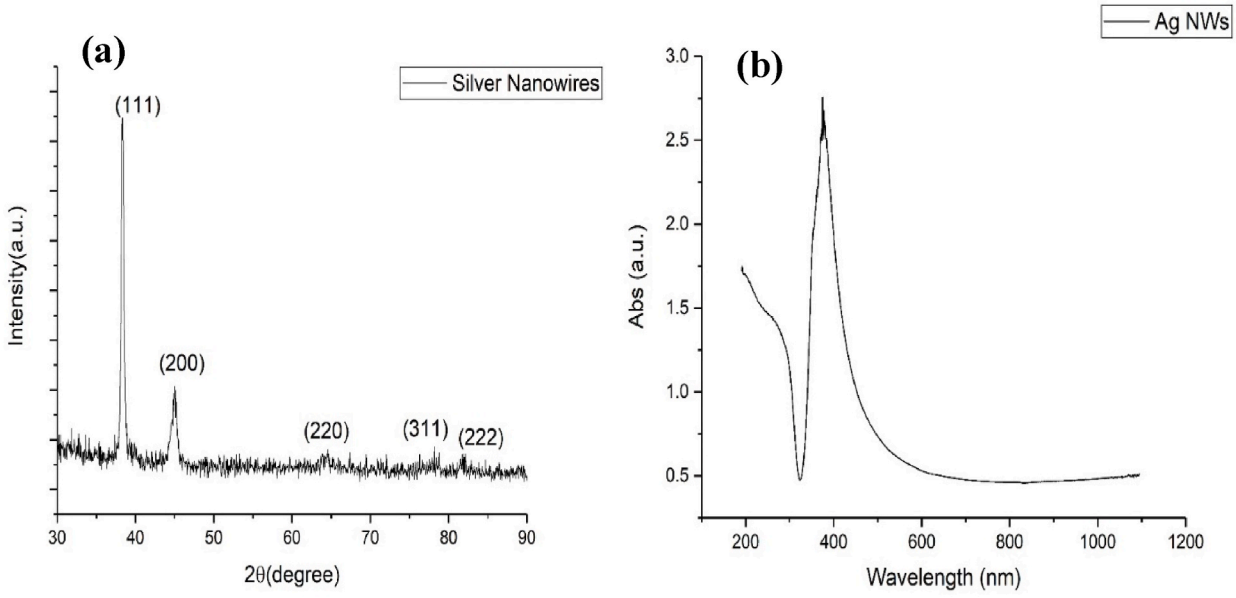

Fig. 1. XRD (a) and UV–visible absorption (b), spectra of silver nanowires.

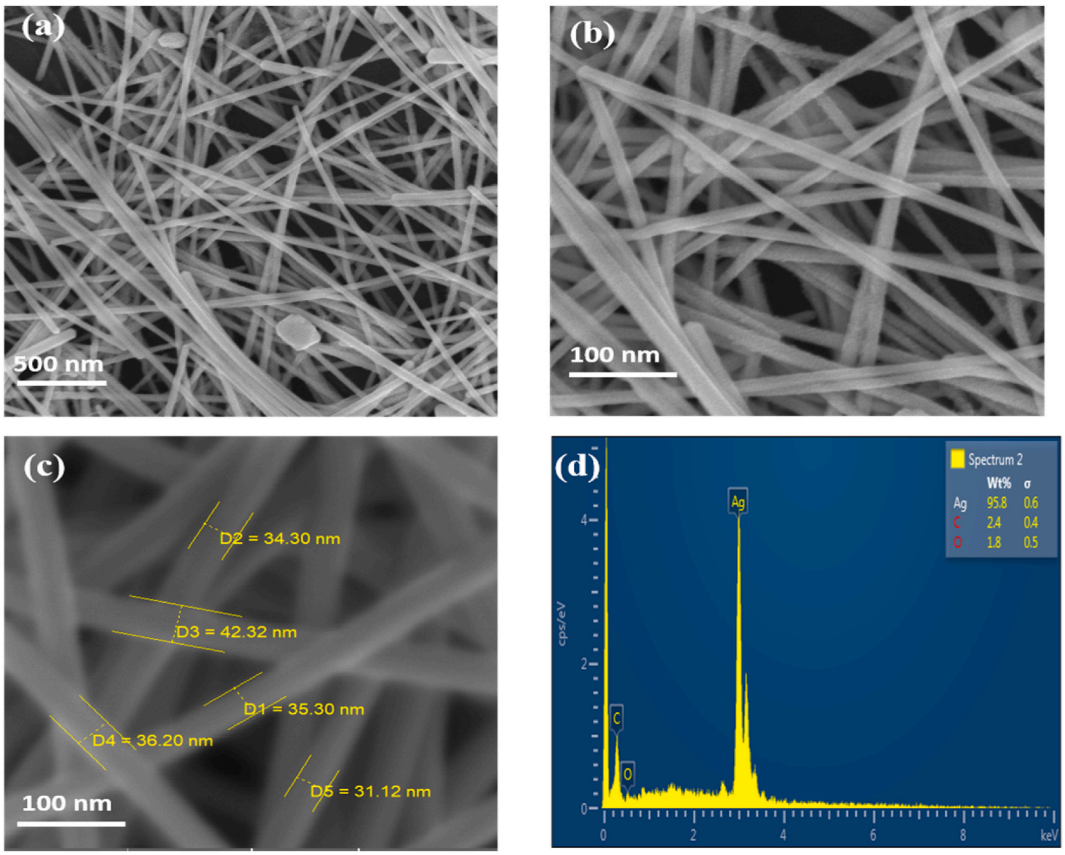

Fig. 2. SEM images of AgNWs at (a) 50kX (b) 100kX (c) 300Kx (d) EDS spectrum of AgNWs.

its lightweight (density~1.2 g/cc), relatively less price and easy availability.

The Prusa MKi3 research printer, equipped with a 0.5 mm nozzle, was employed for 3D printing the honeycomb structures. During the printing process, the nozzle temperature is set to 220 °C, while the bed temperature is maintained at 50 °C. These temperature settings ensure proper melting and adhesion of the PLA material to create the desired structure. The physical dimensions of the 3D printed honeycomb structure, as well as the associated nomenclature, are provided in a table-1 and are visually depicted in a Figure-3.

2.5. Spray coating of AgNWs on honeycomb structures

An aqueous solution containing AgNWs was prepared at a concentration of approximately 10 mg/ml. This solution was then sprayed onto 3D printed structures using a commercial pneumatic spray gun, operating at 5psi pressure, to form a conductive layer of AgNWs on the surface. Subsequently, the coated samples were placed in an oven and dried overnight at a temperature of 40 °C. The coating amount of AgNWs was monitored by measuring the sheet resistance of the samples, which served as an indicator for the thickness of the AgNWs layer. All samples were coated with same amount of AgNWs to achieve sheet resistance of ~1 Ω/square.

Table 1
Dimension parameters of 3D printed honeycomb structures.

	S-1	S-2	S-3	S-4	S-5
Cell size "w" (mm)	10	8	6	4	2
Height "h"(mm)	3	3	3	3	3
Wall thickness "w2" (mm)	1	1	1	1	1
Weight (gm)	~0.61	~0.64	~0.69	~0.76	~0.88
l*s (mm)	22.86*10.16	22.86*10.16	22.86*10.16	22.86*10.16	22.86*10.16

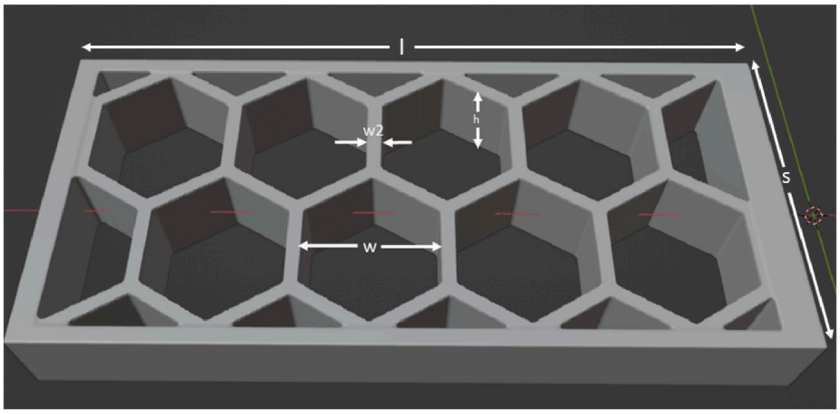

Fig. 3. Honeycomb structure.

3. EMI shielding analysis

3.1. EMI shielding theory

Shielding efficiency of a material is define as decrease in the power of an electromagnetic wave at a point in space after a barrier is introduced between the source at that point [82]. The total shielding effectiveness (SET) of a material can be determined by ratio of incident to transmitted power and for convenience is often represented in logarithmic scale due to large dynamic ranges of power, as given in equation (1). The incident power includes reflected, absorbed and transmitted powers through the shield. The reflected power, SE_R, is mainly produced by free charges at the surface (SE_R) and by multiple reflections (SE_{MR}) from the associated consecutive layers inside the material, if the shield has multi-layered structure. Shielding through absorption (SE_A) is due to dielectric, magnetic and conductive losses in the material. Total shielding effectiveness (SE) can be shown as [83,84].

$$SE_T = 10 \log \left(\frac{P_{out}}{P_{in}} \right) \tag{1}$$

And can be calculated from S-parameters as follow:

$$\text{Power transmitted} = SE_T(dBs) = 10 \log (T) = 10 \log \left(S_{21}^2 \right)$$

$$\text{Power reflected} = SE_R(dBs) = 10 \log (R) = 10 \log \left(S_{11}^2 \right)$$

$$\text{Power absorbed} = SE_A(dBs) = 10 \log(A) = 10 \log (1 - T - R) = 10 \log \left(1 - S_{11}^2 - S_{21}^2 \right)$$

T, R and *A* are coefficients, showing the ratio of power transmitted, reflected, and absorbed to the power incident respectively and *SE* represents respective coefficients converted to decibel scale, and law of conservation of energy requires [24]:

$$R + T + A = 1 \tag{2}$$

In experimental setup to measure the shielding efficiency of a material, SE_{MR} is discussed as a phenomenon which contributes to absorption and/or reflection of the EM wave inside the medium and cannot be measured directly by S-parameters.

It is well established fact that EMI shielding performance of the shield is directly related to its electrical conductivity. Theoretically, SE_T of electrically conductive materials can also be expressed in Simon formalism [85].

$$SE_T = 50 + 10 \log \left(\frac{\sigma}{f} \right) + 1.7t \left(\sqrt{\sigma f} \right)$$

Where,

σ = electrical conductivity
f = frequency of EM waves
t = thickness of the shield.

So it is evident that with increase in electrical conductivity, shielding effectiveness of the material also increases. EMI shielding of the flat conductive materials are mostly due to the reflection of the EM wave from the surface, but when the structure is specially engineered to trap or to enhance the multiple reflection of EM waves, then absorption can be a leading contributing factor to SE_T. In our case, although the surface of the structures is conductive due to spray coating of AgNWs but the honeycomb structure as well as grid pattern of AgNWs facilitate the multiple reflection and trapping of EM waves which in turn contribute to the absorption of EM energy.

3.2. EMI shielding results

EMI shielding measurements were conducted using a Vector Network Analyzer (VNA), ZNB 40 (10 MHz–40 GHz), manufactured by Rohde & Schwarz, employing the waveguide method, as shown in Figure (4). Data is obtained from the machine in the form of S-parameters which give angle and magnitude of the reflected and transmitted electric fields and then plotted and analyzed in the Origin software. The shielding assessment of the samples covered a frequency range of 8.2 GHz–12.4 GHz, specifically within the X-band utilizing WR90 waveguide, at a signal strength of −10 dBm. The prepared samples were sequentially placed in the waveguide's sample holder, with S-parameters recorded for each sample. Figure (5) illustrates the transmission (SE_T), reflection (SE_R), and percentage absorption values for the samples, all samples show the absorption as the primary phenomenon of shielding of EM waves. Notably, a reduction in honeycomb size from 10 mm to 2 mm resulted in an increased shielding effectiveness, peaking at 35 dB for sample S-5. All samples, except for sample S-1, displayed approximately 70 % absorption of the incident wave due to the confinement of electromagnetic waves within the honeycomb cell as well as due to AgNWs. It is evident from our study that up to 70 % of the EM waves are absorbed inside the structures, which may be attributed to two leading causes 1) honeycomb openings with 3 mm height, which act as traps for incoming EM waves and hence waves undergo multiple reflection inside the walls of the HC, EM energy is absorbed at each reflection site. 2) AgNWs, which instead of a continuous metallic surface make grid like pattern with microscopic pinholes and openings. This grid like pattern may also contribute to the absorption of the EM waves due to peculiar reflection sites. The enhanced shielding performance is due to continuous conductive grid pattern made by AgNWs on the surface of the structures. The SE_T results demonstrated a significant improvement in shielding efficiency when the honeycomb cell size decreased from 10 mm to 8 mm, followed by 6 mm, this is attributed to the change in wavelength to cell size ratio (λ:w). However, further reduction in cell size to 4 mm and 2 mm only yielded marginal improvements in shielding efficiency due to fact that $\lambda \gg$w. By increasing the coating layer of AgNWs, the surface resistivity of the samples can be further reduced below 1 Ω/square, which will eventually give rise to.

Shielding performance. Figure (5-b) represents the power reflected from samples in decibels scale, indicating a consistent value for the reflected power except in the case of sample S-1. For sample S-1, reflected power decreases as frequency increases, and can be attributed to transmission of almost all incident power through the sample at higher frequencies due to small wavelength to cell size ratio ($<\lambda$: w). It is worth noting that the shielding effectiveness decreased across all samples with increase in frequency, which is due to the diminishing wavelength to cell size ratio (λ: w).

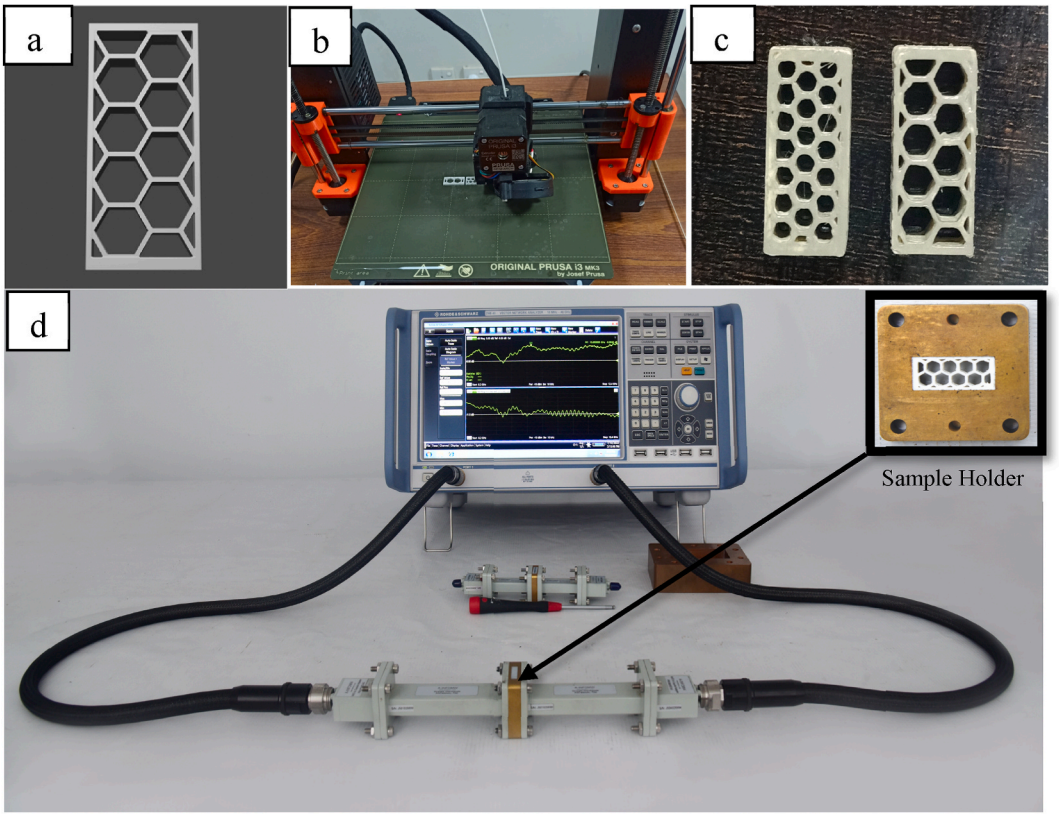

Fig. 4. Steps involve in the fabrication of honeycomb structure a) 3D design modeling and slicing b) 3D printing c) spray coating of AgNWs d) measurement of EMI shielding.

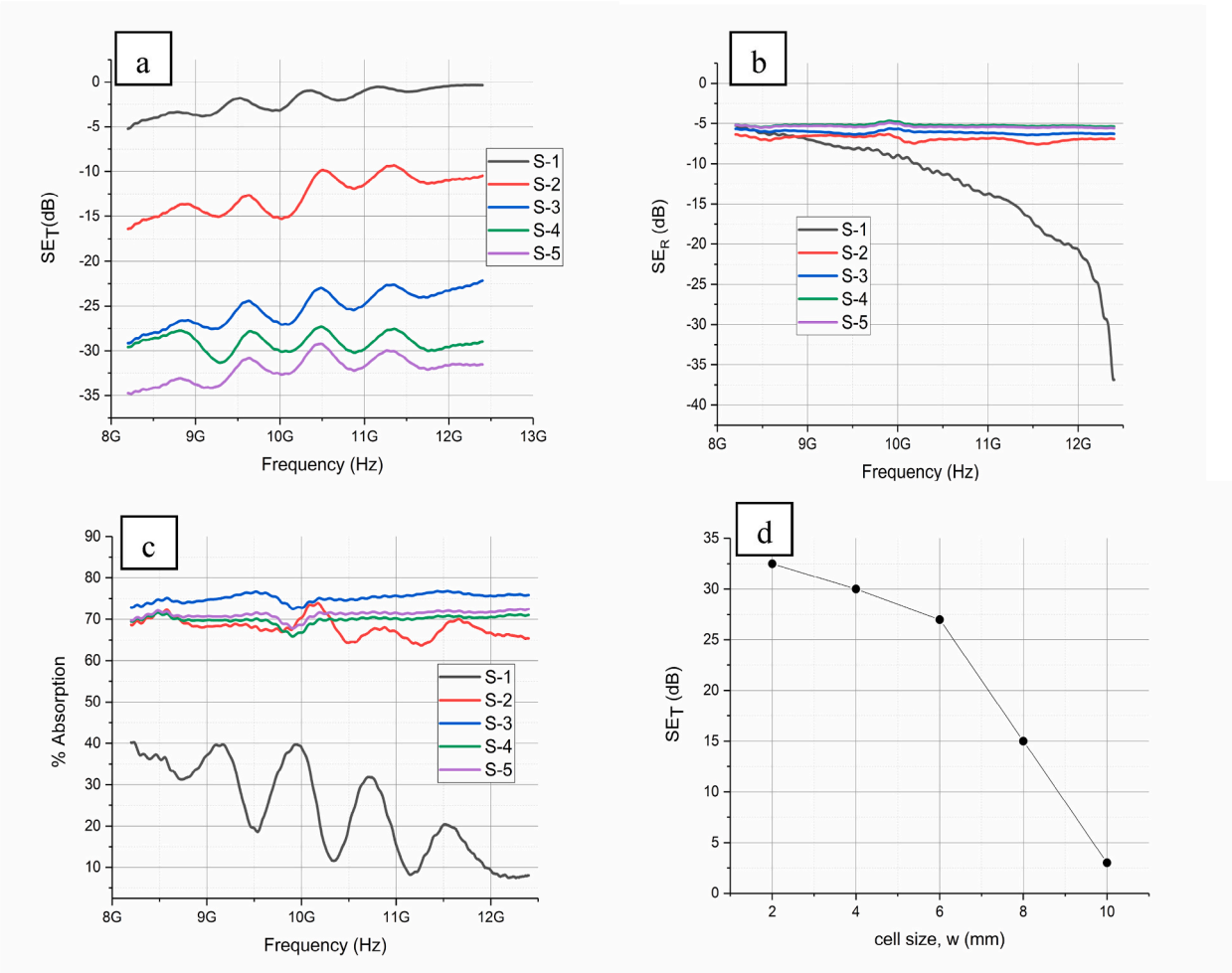

Fig. 5. EMI shielding results in X-band. a) transmitted power b) reflected power c) percentage of power absorbed inside structures and d) variation of SE_T with honeycomb cell size at 10 GHz.

4. Conclusion

This study presents a novel approach for the development of lightweight 3D printed structures that serve a dual purpose of providing EMI shielding as well as air ventilation for cooling purpose of electronic components. The technique employed involves utilizing the Fused Deposition Modeling (FDM) method to fabricate Polylactic Acid (PLA) made honeycomb structures, followed by a spray coating of a AgNWs solution to create a conductive surface. The incorporation of AgNWs with their high aspect ratio contributes to achieving an impressive surface conductivity of 1 Ω/square. Experimental testing using the VNA waveguide method in the X-band demonstrates the exceptional EMI shielding capabilities of the developed samples. These samples exhibit efficient EMI shielding, providing attenuation of up to 35 dB, equivalent to an impressive ~99.97 % reduction in electromagnetic interference. Moreover, the shielding provided by samples is primarily absorption-based, with up to 75 % absorption of power within the structure.

The findings of this study have promising implications for industries and sectors where simultaneous air venting and EMI shielding are critical. The combination of 3D printing technology with a conductive silver nanowire spray enables the creation of complex and customizable structures with efficient EMI shielding capabilities. Future research in this field can explore further advancements in materials and manufacturing techniques, contributing to the development of innovative solutions for EMI shielding in various sectors, including electronics, telecommunications, and related applications.

Data availability

Date will be made available on reasonable request.

CRediT authorship contribution statement

Raheel Abbas: Writing – original draft, Methodology, Conceptualization, Investigation. **Ubaid ur Rehman:** Writing – original draft, Methodology, Investigation, Data curation. **Ahmed bilal:** Software, Investigation, Formal analysis. **Numrah Sultan:** Investigation, Formal analysis. **Uzma Ghazanfar:** Visualization, Supervision, Formal analysis. **Tahir Ali:** Methodology, Formal analysis. **Muhammad Nadeem:** Writing – review & editing, Supervision, Resources, Project administration.

Declaration of generative AI and AI-assisted technologies in the writing process

During the preparation of this work the authors utilized Chat GPT-3, in order to enhance English grammar and readability. After using this tool/service, the authors reviewed and edited the content as needed and take full responsibility for the content of the publication.

Declaration of competing interest

The authors declare that they have no known competing financial interests or personal relationships that could have appeared to influence the work reported in this paper.

Acknowledgement

This research did not receive any specific grant from funding agencies in the public, commercial, or not-for-profit sectors.

References

[1] R. Wilson, G. George, K. Joseph, An introduction to materials for potential EMI shielding applications: status and future, Materials for Potential EMI Shielding Applications (2020) 1–8. Elsevier.
[2] A. Kausar, I. Ahmad, Conducting polymer nanocomposites for electromagnetic interference shielding—radical developments, Journal of Composites Science 7 (6) (2023) 240.
[3] Y.-K. Li, P.-Y. Du, Z.-X. Wang, H.-D. Huang, L.-C. Jia, Aramid nanofiber-induced assembly of graphene nanosheets toward highly thermostable and freestanding films for electromagnetic interference shielding, Compos. Appl. Sci. Manuf. 160 (2022) 107063.
[4] S. Geetha, K. Satheesh Kumar, C.R. Rao, M. Vijayan, D. Trivedi, EMI shielding: methods and materials—a review, J. Appl. Polym. Sci. 112 (4) (2009) 2073–2086.
[5] A.U. Rehman, M. Atif, U. ur Rehman, H. Wahab, F.C.-C. Ling, W. Khalid, A. Ul-Hamid, Z. Ali, M. Nadeem, Tuning the magnetic and dielectric properties of Fe3O4 nanoparticles for EMI shielding applications by doping a small amount of Ni2+/Zn2+, Mater. Today Commun. 34 (2023) 105454.
[6] Y. Guo, N.R. Vokhidova, Q. Wang, B. Lan, Y. Lu, Lightweight and thermal insulation fabric-based composite foam for high-performance electromagnetic interference shielding, Mater. Chem. Phys. 303 (2023) 127787.
[7] H. Abbasi, M. Antunes, J.I. Velasco, Recent advances in carbon-based polymer nanocomposites for electromagnetic interference shielding, Prog. Mater. Sci. 103 (2019) 319–373.
[8] Y. Xu, Y. Yang, D.-X. Yan, H. Duan, G. Zhao, Y. Liu, Flexible and conductive polyurethane composites for electromagnetic shielding and printable circuit, Chem. Eng. J. 360 (2019) 1427–1436.
[9] A. Iqbal, P. Sambyal, C.M. Koo, 2D MXenes for electromagnetic shielding: a review, Adv. Funct. Mater. 30 (47) (2020) 2000883.
[10] Y. Yao, S. Jin, H. Zou, L. Li, X. Ma, G. Lv, F. Gao, X. Lv, Q. Shu, Polymer-based lightweight materials for electromagnetic interference shielding: a review, J. Mater. Sci. 56 (11) (2021) 6549–6580.
[11] P. Kallambadi Sadashivappa, R. Venkatachalam, R. Pothu, R. Boddula, P. Banerjee, R. Naik, A.B. Radwan, N. Al-Qahtani, Progressive review of functional nanomaterials-based polymer nanocomposites for efficient EMI shielding, Journal of Composites Science 7 (2) (2023) 77.
[12] A.U. Rehman, M. Atif, S. Baqi, A. Ul-Hamid, U. ur Rehman, W. Khalid, Z. Ali, F.C.-C. Ling, M. Nadeem, Enhancement in the electromagnetic shielding properties of doped M0. 01Fe2. 99O4 magnetite nanoparticles (M= Mn2+, Ni2+, Cu2+, Zn2+), J. Alloys Compd. (2023) 171051.
[13] J. Lou, A. Bhobe, J. Pianin, Air Vent with Openings of Random Size and Location for Improved EMI Shielding and Air Flow, 2022, pp. 481–484.
[14] S.P. Rea, D. Linton, E. Orr, J. McConnell, EMI suppression in an aircraft cooling vent, IEE Proc. Microw. Antenn. Propag. 152 (2) (2005) 57.
[15] X.-z. Jin, Z.-y. Yang, C.-h. Huang, J.-h. Yang, Y. Wang, PEDOT: PSS/MXene/PEG composites with remarkable thermal management performance and excellent HF-band & X-band electromagnetic interference shielding efficiency for electronic packaging, Chem. Eng. J. 448 (2022) 137599.
[16] L.-C. Jia, Z.-X. Wang, L. Wang, J.-F. Zeng, P.-Y. Du, Y.-F. Yue, L.-H. Zhao, S.-L. Jia, Self-standing boron nitride bulks enabled by liquid metals for thermal management, Mater. Horiz. 10 (12) (2023) 5656–5665.
[17] Y.-K. Li, W.-J. Li, Z.-X. Wang, P.-Y. Du, L. Xu, L.-C. Jia, D.-X. Yan, High-efficiency electromagnetic interference shielding and thermal management of high-graphene nanoplate-loaded composites enabled by polymer-infiltrated technique, Carbon 211 (2023) 118096.
[18] L.-C. Jia, Y.-F. Yue, J. Zeng, Z. Wang, R.-P. Nie, L. Xu, D.-X. Yan, Z.-M. Li, A review on thermal and electrical behaviours of liquid metal-based polymer composites, J. Mater. Chem. C 11 (2023) 12807–12827.
[19] I.B. Basyigit, H. Dogan, S. Helhel, The effect of aperture shape, angle of incidence and polarization on shielding effectiveness of metallic enclosures, J. Microw. Power Electromagn. Energy 53 (2) (2019) 115–127.
[20] L.-H. Zhao, L. Wang, Y.-F. Jin, J.-W. Ren, Z. Wang, L.-C. Jia, Simultaneously improved thermal conductivity and mechanical properties of boron nitride nanosheets/aramid nanofiber films by constructing multilayer gradient structure, Compos. B Eng. 229 (2022) 109454.
[21] D.R. White, M. Mardiguian, A Handbook Series on Electromagnetic Interference and Compatibility: Electromagnetic Shielding, Interference Control Technologies, 1988.
[22] S. Güler, An investigation on electromagnetic shielding effectiveness of metallic enclosure depending on aperture position, J. Microw. Power Electromagn. Energy 57 (2) (2023) 129–145.
[23] K. Ji, H. Zhao, Z. Huang, Z. Dai, Performance of open-cell foam of Cu–Ni alloy integrated with graphene as a shield against electromagnetic interference, Mater. Lett. 122 (2014) 244–247.
[24] X.C. Tong, Advanced Materials and Design for Electromagnetic Interference Shielding, CRC press, 2016.
[25] I.B. Basyigit, H. Dogan, The analytical and artificial intelligence methods to investigate the effects of aperture dimension ratio on electrical shielding effectiveness, International Journal of Electronics and Telecommunications 65 (3) (2019) 359–365.
[26] L.-C. Jia, Y.-F. Jin, J.-W. Ren, L.-H. Zhao, D.-X. Yan, Z.-M. Li, Highly thermally conductive liquid metal-based composites with superior thermostability for thermal management, J. Mater. Chem. C 9 (8) (2021) 2904–2911.

[27] H. Mei, X. Zhao, S. Zhou, D. Han, S. Xiao, L. Cheng, 3D-printed oblique honeycomb Al2O3/SiCw structure for electromagnetic wave absorption, Chem. Eng. J. 372 (2019) 940–945.
[28] B. Berman, 3-D printing: the new industrial revolution, Bus. Horiz. 55 (2) (2012) 155–162.
[29] S. Brischetto, R. Torre, Honeycomb sandwich specimens made of PLA and produced via 3D FDM printing process: an experimental study, Journal of Aircraft and Spacecraft Technology 4 (1) (2020) 54–69.
[30] K.V. Wong, A. Hernandez, A review of additive manufacturing, ISRN Mechanical Engineering 2012 (2012) 1–10.
[31] S. Park, W. Shou, L. Makatura, W. Matusik, K.K. Fu, 3D printing of polymer composites: materials, processes, and applications, Matter 5 (1) (2022) 43–76.
[32] A. Jandyal, I. Chaturvedi, I. Wazir, A. Raina, M.I.U. Haq, 3D printing–A review of processes, materials and applications in industry 4.0, Sustainable Operations and Computers 3 (2022) 33–42.
[33] N. Shahrubudin, T.C. Lee, R. Ramlan, An overview on 3D printing technology: technological, materials, and applications, Procedia Manuf. 35 (2019) 1286–1296.
[34] C. Schubert, M.C. Van Langeveld, L.A. Donoso, Innovations in 3D printing: a 3D overview from optics to organs, Br. J. Ophthalmol. 98 (2) (2014) 159–161.
[35] R. Allouzi, W. Al-Azhari, R. Allouzi, Conventional construction and 3D printing: a comparison study on material cost in Jordan, J. Eng. 2020 (2020) 1–14.
[36] E. MacDonald, R. Wicker, Multiprocess 3D printing for increasing component functionality, Science 353 (6307) (2016) aaf2093.
[37] J. Feng, J. Fu, Z. Lin, C. Shang, B. Li, A review of the design methods of complex topology structures for 3D printing, Visual Computing for Industry, Biomedicine, and Art 1 (1) (2018) 1–16.
[38] S. Verma, M. Dhangar, M. Mili, H. Bajpai, U. Dwivedi, N. Kumari, M.A. Khan, H.N. Bhargaw, S.A.R. Hashmi, A.K. Srivastava, Review on engineering designing of electromagnetic interference shielding materials using additive manufacturing, Polym. Compos. 43 (7) (2022) 4081–4099.
[39] Z. Viskadourakis, K. Vasilopoulos, E. Economou, C.M. Soukoulis, G. Kenanakis, Electromagnetic shielding effectiveness of 3D printed polymer composites, Appl. Phys. A 123 (2017) 1–7.
[40] Q. Lv, X. Tao, S. Shi, Y. Li, N. Chen, From materials to components: 3D-printed architected honeycombs toward high-performance and tunable electromagnetic interference shielding, Compos. B Eng. 230 (2022) 109500.
[41] B. Uspensky, K. Avramov, I. Derevianko, O. Polishchuk, O. Salenko, Stiffness and fatigue of sandwich plates with honeycomb core manufactured by fused deposition modeling. International Conference on Smart Technologies in Urban Engineering, Springer, 2022, pp. 477–488.
[42] S. Gohar, G. Hussain, A. Ali, H. Ahmad, Mechanical performance of honeycomb sandwich structures built by FDM printing technique, J. Thermoplast. Compos. Mater. 36 (1) (2021) 182–200.
[43] P. Song, Z. Ma, H. Qiu, Y. Ru, J. Gu, High-efficiency electromagnetic interference shielding of rGO@FeNi/epoxy composites with regular honeycomb structures, Nano-Micro Lett. 14 (1) (2022) 51.
[44] P. Song, C. Liang, L. Wang, H. Qiu, H. Gu, J. Kong, J. Gu, Obviously improved electromagnetic interference shielding performances for epoxy composites via constructing honeycomb structural reduced graphene oxide, Compos. Sci. Technol. 181 (2019) 107698.
[45] P. Song, Z. Ma, H. Qiu, Y. Ru, J. Gu, High-efficiency electromagnetic interference shielding of rGO@ FeNi/epoxy composites with regular honeycomb structures, Nano-Micro Lett. 14 (1) (2022) 51.
[46] J.-M. Thomassin, C. Jérôme, T. Pardoen, C. Bailly, I. Huynen, C. Detrembleur, Polymer/carbon based composites as electromagnetic interference (EMI) shielding materials, Mater. Sci. Eng. R Rep. 74 (7) (2013) 211–232.
[47] J. Subramanian, V.K. Selvaraj, K.K. Saxena, E. Jayamani, R. Singh, C. Prakash, D. Buddhi, 3D-printed honeycomb structure filled with nanofillers for efficient electromagnetic interference shielding performance, Proc. IME E J. Process Mech. Eng. (2024) 09544089231221677.
[48] M.H. Al-Saleh, U. Sundararaj, Electromagnetic interference shielding mechanisms of CNT/polymer composites, Carbon 47 (7) (2009) 1738–1746.
[49] R.J. Chandra, B. Shivamurthy, S.D. Kulkarni, M.S. Kumar, Hybrid polymer composites for EMI shielding application-a review, Mater. Res. Express 6 (8) (2019) 082008.
[50] X. Wang, Z. Lei, X. Ma, G. He, T. Xu, J. Tan, L. Wang, X. Zhang, L. Qu, X. Zhang, A lightweight MXene-coated nonwoven fabric with excellent flame retardancy, EMI shielding, and electrothermal/photothermal conversion for wearable heater, Chem. Eng. J. 430 (2022) 132605.
[51] V.-T. Nguyen, Q.-D. Nguyen, B.K. Min, Y. Yi, C.-G. Choi, Ti3C2Tx MXene/carbon nanotubes/waterborne polyurethane based composite ink for electromagnetic interference shielding and sheet heater applications, Chem. Eng. J. 430 (2022) 133171.
[52] A. Perera, K. Song, S. Umezu, H. Sato, Recent progress in functionalized plastic 3D printing in creation of metallized architectures, Mater. Des. (2023) 112044.
[53] M.-Z. Chen, L.-Y. Wang, G. Liu, C.-Q. Ge, D.-C. Li, Q.-X. Liang, Lightweight broadband microwave absorbing metamaterial with CB-ABS composites fabricated by 3D printing, Chin. Phys. B 32 (4) (2023) 048103.
[54] F. Shahzad, M. Alhabeb, C.B. Hatter, B. Anasori, S. Man Hong, C.M. Koo, Y. Gogotsi, Electromagnetic interference shielding with 2D transition metal carbides (MXenes), Science 353 (6304) (2016) 1137–1140.
[55] Y. Yang, M.C. Gupta, K.L. Dudley, R.W. Lawrence, A comparative study of EMI shielding properties of carbon nanofiber and multi-walled carbon nanotube filled polymer composites, J. Nanosci. Nanotechnol. 5 (6) (2005) 927–931.
[56] Z.-X. Wang, P.-Y. Du, W.-J. Li, J.-H. Meng, L.-H. Zhao, S.-L. Jia, L.-C. Jia, Highly rapid-response electrical heaters based on polymer-infiltrated carbon nanotube networks for battery thermal management at subzero temperatures, Compos. Sci. Technol. 231 (2023) 109796.
[57] L. Yang, X. Liu, Y. Xiao, B. Liu, Z. Xue, Y. Wang, Additive manufacturing of carbon nanotube/polylactic acid films with efficient electromagnetic interference shielding and electrical heating performance via fused deposition modeling, Synth. Met. 293 (2023) 117258.
[58] Z. Manzoor, M.T. Ghasr, K.M. Donnell, Microwave Characterization of 3D Printed Conductive Composite Materials, 2018, pp. 1–5.
[59] H. Zhang, X. Zhou, Y. Gao, L. Wu, L. Lyu, Microwave absorption and bending properties of three-dimensional gradient honeycomb woven composites, Polym. Compos. 44 (2) (2023) 1201–1212.
[60] Y. Zhan, C. Santillo, Y. Meng, M. Lavorgna, Recent advances and perspectives on silver-based polymer composites for electromagnetic interference shielding, J. Mater. Chem. C 11 (2023) 859–892.
[61] C. Levard, E.M. Hotze, G.V. Lowry, G.E. Brown Jr., Environmental transformations of silver nanoparticles: impact on stability and toxicity, Environ. Sci. Technol. 46 (13) (2012) 6900–6914.
[62] H. Jiang, K.-S. Moon, J. Lu, C. Wong, Conductivity enhancement of nano silver-filled conductive adhesives by particle surface functionalization, J. Electron. Mater. 34 (2005) 1432–1439.
[63] K.M. Abou El-Nour, A.a. Eftaiha, A. Al-Warthan, R.A. Ammar, Synthesis and applications of silver nanoparticles, Arab. J. Chem. 3 (3) (2010) 135–140.
[64] R. Ravindren, S. Mondal, K. Nath, N.C. Das, Prediction of electrical conductivity, double percolation limit and electromagnetic interference shielding effectiveness of copper nanowire filled flexible polymer blend nanocomposites, Compos. B Eng. 164 (2019) 559–569.
[65] S. Li, K. Qian, S. Thaiboonrod, H. Wu, S. Cao, M. Miao, L. Shi, X. Feng, Flexible multilayered aramid nanofiber/silver nanowire films with outstanding thermal durability for electromagnetic interference shielding, Compos. Appl. Sci. Manuf. 151 (2021) 106643.
[66] B. Zhou, M. Su, D. Yang, G. Han, Y. Feng, B. Wang, J. Ma, J. Ma, C. Liu, C. Shen, Flexible MXene/silver nanowire-based transparent conductive film with electromagnetic interference shielding and electro-photo-thermal performance, ACS Appl. Mater. Interfaces 12 (36) (2020) 40859–40869.
[67] X. Zhu, J. Xu, F. Qin, Z. Yan, A. Guo, C. Kan, Highly efficient and stable transparent electromagnetic interference shielding films based on silver nanowires, Nanoscale 12 (27) (2020) 14589–14597.
[68] D. Fu, R. Yang, Y. Wang, R. Wang, F. Hua, Silver nanowire synthesis and applications in composites: progress and prospects, Advanced Materials Technologies 7 (11) (2022) 2200027.
[69] D. Tan, C. Jiang, Q. Li, S. Bi, J. Song, Silver nanowire networks with preparations and applications: a review, J. Mater. Sci. Mater. Electron. 31 (2020) 15669–15696.
[70] J. Jung, H. Lee, I. Ha, H. Cho, K.K. Kim, J. Kwon, P. Won, S. Hong, S.H. Ko, Highly stretchable and transparent electromagnetic interference shielding film based on silver nanowire percolation network for wearable electronics applications, ACS Appl. Mater. Interfaces 9 (51) (2017) 44609–44616.

[71] X. Hong, W. Zhao, R. Yu, Q. Wang, F. Zeng, Y. Tao, Z. Jin, C. Zhu, Multifunctional silver nanowire coated fabric capable of electrothermal, resistance temperature-sensitivity, electromagnetic interference shielding, and strain sensing, J. Ind. Textil. 51 (4_suppl) (2022) 6153S–6172S.
[72] X. Zhang, Y. Zhong, Y. Yan, Electrical, mechanical, and electromagnetic shielding properties of silver nanowire-based transparent conductive films, Phys. Status Solidi 215 (14) (2018) 1800014.
[73] D.G. Kim, J.H. Choi, D.-K. Choi, S.W. Kim, Highly bendable and durable transparent electromagnetic interference shielding film prepared by wet sintering of silver nanowires, ACS Appl. Mater. Interfaces 10 (35) (2018) 29730–29740.
[74] Y. Li, S. Guo, H. Yang, Y. Chao, S. Jiang, C. Wang, One-step synthesis of ultra-long silver nanowires of over 100 mum and their application in flexible transparent conductive films, RSC Adv. 8 (15) (2018) 8057–8063.
[75] Z. Wang, J. Liu, X. Chen, J. Wan, Y. Qian, A simple hydrothermal route to large-scale synthesis of uniform silver nanowires, Chem.–Eur. J. 11 (1) (2005) 160–163.
[76] B. Bari, J. Lee, T. Jang, P. Won, S.H. Ko, K. Alamgir, M. Arshad, L.J. Guo, Simple hydrothermal synthesis of very-long and thin silver nanowires and their application in high quality transparent electrodes, J. Mater. Chem. A 4 (29) (2016) 11365–11371.
[77] S. Fahad, H. Yu, L. Wang, M. Haroon, R.S. Ullah, A. Nazir, K.-u.-R. Naveed, T. Elshaarani, A. Khan, Recent progress in the synthesis of silver nanowires and their role as conducting materials, J. Mater. Sci. 54 (2019) 997–1035.
[78] M.R. Azani, A. Hassanpour, Synthesis of silver nanowires with controllable diameter and simple tool to evaluate their diameter, concentration and yield, ChemistrySelect 4 (9) (2019) 2716–2720.
[79] H. Mao, J. Feng, X. Ma, C. Wu, X. Zhao, One-dimensional silver nanowires synthesized by self-seeding polyol process, J. Nanoparticle Res. 14 (2012) 1–15.
[80] D. Chen, X. Qiao, X. Qiu, J. Chen, R. Jiang, Large-scale synthesis of silver nanowires via a solvothermal method, J. Mater. Sci. Mater. Electron. 22 (2011) 6–13.
[81] C. Chen, L. Wang, G. Jiang, J. Zhou, X. Chen, H. Yu, Q. Yang, Study on the synthesis of silver nanowires with adjustable diameters through the polyol process, Nanotechnology 17 (15) (2006) 3933.
[82] M. Jaroszewski, S. Thomas, A.V. Rane, Advanced Materials for Electromagnetic Shielding: Fundamentals, Properties, and Applications, 2018.
[83] D. Jiang, V. Murugadoss, Y. Wang, J. Lin, T. Ding, Z. Wang, Q. Shao, C. Wang, H. Liu, N. Lu, R. Wei, A. Subramania, Z. Guo, Electromagnetic interference shielding polymers and nanocomposites - a review, Polym. Rev. 59 (2) (2019) 280–337.
[84] X.-Y. Wang, S.-Y. Liao, Y.-J. Wan, P.-L. Zhu, Y.-G. Hu, T. Zhao, R. Sun, C.-P. Wong, Electromagnetic interference shielding materials: recent progress, structure design, and future perspective, J. Mater. Chem. C 10 (1) (2022) 44–72.
[85] H.W. Ott, Electromagnetic Compatibility Engineering, John Wiley & Sons, 2011.